Proceedings of the 6th Nordic Signal Processing Symposium - NORSIG 2004
June 9 - 11, 2004
Espoo, Finland

Comparison of Continuous- and Discrete-Time Modelling of Polynomial-Based Interpolation Filters

Vesa Lehtinen, Djordje Babic, and Markku Renfors

Tampere University of Technology
Institute of Communications Engineering
P.O. Box 553, FIN-33101 Tampere, FINLAND
Email: {vesa.lehtinen,markku.renfors}@tut.fi, djordje.babic@ieee.org

ABSTRACT

Polynomial-based interpolation filters provide a flexible means for arbitrary and asynchronous sample rate conversion. They can be modelled with a continuous-time piecewise-polynomial impulse response. In sample rate conversion by rational factors, however, only discrete points of the impulse response affect the output signal. This leads to a discrete-time model of the interpolator. In this paper, properties of the continuous- and discrete-time models in optimisation of filters for sample rate conversion are discussed and compared so that the best model can be chosen for each filter design task. Interpolators optimised using the discrete-time model are optimal when a rational conversion factor is fixed. However, interpolators optimised using the continuous-time model can be more robust against changes of the conversion factor, which property is useful in applications that require flexibility.

1. INTRODUCTION

Sample rate conversion (SRC) by rational factors is needed in, e.g., digital multimode communication receivers, where the ratios between the sampling rate of the analogue-to-digital converter and the symbol/chip rates of different communication standards cannot all be integers in practise. Another typical application is in digital audio systems, where rational SRC is needed in interconnection of devices that conform to different standards.

The most straightforward way to realise rational SRC is to perform up- and downsampling by integer factors and anti-image/antialias filtering between them. The structure can be optimised by avoiding multiplications by zero samples and computation of unused output samples. [1, pp. 88–91]. Polynomial-based interpolation filters provide a more flexible approach that is often also more efficient, and most importantly, is feasible also when the SRC factor is a ratio of two large integers or even irrational. For rational SRC, these filters have been optimised using both continuous-time (CT) and discrete-time (DT) models. These models have benefits and drawbacks that have not been sufficiently analysed before. The purpose of this paper is to give the reader insight to the models and allow the selection of the best model for each filter design task.

This work was carried out in the project "Advanced Signal Processing Techniques for Future Wireless Communications Transceivers" supported by the Academy of Finland. The work was also supported by Tampere International School in Information Science and Engineering (TISE) and Nokia Foundation.

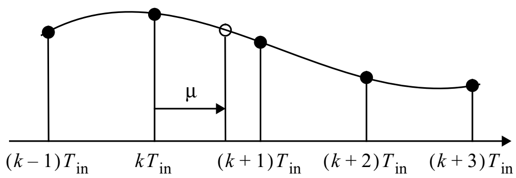

Fig. 1. The principle of interpolation filtering. The continuous-time signal represented by a discrete-time sequence is reconstructed at the time instants $(k+\mu)T_{\text{in}}$.

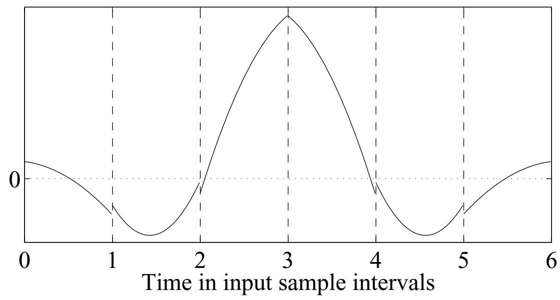

Fig. 2. A typical CT impulse response of a polynomial-based interpolation filter.

2. POLYNOMIAL-BASED INTERPOLATION AND THE FARROW STRUCTURE

The principle of interpolation filtering is illustrated in Fig. 1. A continuous-time signal is reconstructed at desired time instants from a sequence of its samples. As parameters, the interpolation filter is given the input sample index k and the fractional interval $\mu \in [0, 1)$ for each desired output sample. Polynomial-based interpolation filters produce a piecewise-polynomial reconstruction of the signal. A typical CT impulse response of a polynomial-based interpolation filter is shown in Fig. 2. [2]

The Farrow structure [3], depicted in Fig. 3, is a convenient and efficient implementation form for polynomial-based variable filters, including interpolators. Its impulse response taps are polynomials in a control variable. In interpolation, the control variable is a function

©2004 NORSIG 2004

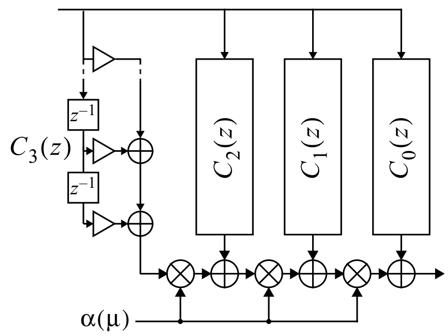

Fig. 3. The Farrow structure. For the Modified Farrow structure, $\alpha(\mu)=2\mu-1$.

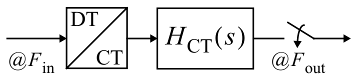

Fig. 4. The continuous-time model for fractional sample rate conversion.

of the fractional interval. A number of modifications have been developed: The Modified Farrow structure improves efficiency by exploiting coefficient symmetry [2]. The transposed Farrow structure [4][5] provides good antialiasing properties for decimation (the original Farrow structure has poor antialiasing performance). Also other variants have been proposed. In this paper, only the Modified and transposed Modified Farrow structure are considered but most of the results apply to other variants as well.

3. INTERPOLATOR MODELS

3.1 Continuous-time model

SRC by any factor can be modelled with the system presented in Fig. 4 [1, pp. 22–29]. The input sample sequence is converted into the equivalent continuous-time train of weighted Dirac impulses, filtered with a CT reconstruction filter and then sampled at the output sample rate. From the frequency-domain point of view, the purpose of the reconstruction filter is to reject images and/ or limit the bandwidth in order to avoid aliasing. A typical CT impulse response is shown in Fig. 2. The CT frequency response is defined as the Fourier transform of the CT impulse response.

3.2 Discrete-time model

In interpolation by a rational factor L/K (with $K<L$) using the Farrow structure, or in decimation by L/K using the transposed Farrow structure, the sequence of μ-values is periodic with periodicity of L and quasiperiodic with quasiperiodicity of L/K. It can be shown that μ takes L different values. [6, p. 20] This leads to the discrete-time model [1, pp. 29–31,39–42][7][6, pp. 20–21] illustrated in Fig. 5. The DT impulse response is obtained by sampling the CT impulse response at intervals of T/L, where T is the output (input) sample interval of the decimator

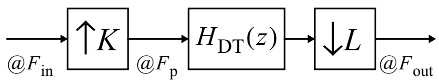

Fig. 5. The discrete-time model for rational decimation.

(interpolator):

$$h_{DT}[n] = h_{CT}\left(\left(\frac{n}{L} + \mu_{bias}\right)T\right), \tag{3.1}$$

where μ_{bias} is a bias used for choosing the sampling phase. The bias has an effect on the magnitude and phase response [8][9]. The DT frequency response is defined as the Fourier transform of the CT impulse response. Calculation of the discrete-time impulse response for different Farrow variants has been discussed in [8]. Notice that the DT model depends on L and μ_{bias}. Moreover, in irrational SRC, μ takes an infinite number of different values, hence the DT model does not exist.

For purposes of Section 4, we define L_T as the target value of L, i.e., the value used when designing the filter. The value of L used in the realisation is denoted by L_R.

4. COMPARISON OF THE MODELS

For comparison, a set of interpolators were optimised for different signal bandwidths, attenuation specifications, and values of L_T. Cases with a single continuous stopband and multiple stopbands (comprised of the bands aliasing to the passband) were considered. In each case, the same subfilter lengths and polynomial degrees were used for the CT design and all target conversion ratios of the DT model, with exceptions explained below. For the DT designs, μ-biasing [9] was used in order to obtain the best performance. The peak stopband ripple levels of the DT frequency responses of a few example filters are shown in Figs. 6–9 as functions of L_R. In the plots, M and N denote the polynomial degree and number of polynomial segments of the filter, respectively. The passband edge f_p is normalised so that unity corresponds to half of the sample rate in the subfilters. Only minimax optimisation was considered in the comparison.

It can be observed that the peak ripple depends on L_R. The reason is that, in the sampler of the CT model, multiple images of a given input frequency alias to the same output frequency. Their phase differences depend only on the filter $H_{CT}(s)$, not on the input phase. The summation of these aliases can be either constructive (deteriorates attenuation) or destructive (improves attenuation) depending on the phase response of the filter. At different values of L_R, the aliasing patterns of images of a given input frequency are different, resulting in different peak ripple levels in the DT model. When L_R approaches infinity, the DT ripple level approaches that of the CT frequency response, whereas the maximum attenuation loss is suffered at the lowest values of L_R. Fig. 10 shows that the value of L_R below which significant attenuation loss occurs is almost independent of the polynomial degree.

When interpolation filters are optimised using the DT model, the destructive summation mentioned above is automatically exploited. This means that the peak ripple level of the CT frequency response may become greater than that of the DT frequency response at L_R=L_T. If L_R is then changed, the higher ripples of the CT response become visible because imaging or aliasing changes. Also the proportions of constructive and destructive summation change. This explains the bad performance of DT-optimised interpolators for $L_R \neq L_T$.

The CT frequency response is nonperiodic. Therefore, an infinite bandwidth must be covered in response analysis. In practise, the magnitude response decays at high frequencies so that frequencies above some limit can be ignored – the introduced error is buried under roundoff errors. However, this limit must be determined in a proper manner in order to prevent overly optimistic approximation.

Because the DT frequency response is periodic, the bandwidth to be covered is always bounded by the intermediate sample rate F_p (or $F_p/2$ for real-valued filters). (F_p is present only in the model, not in the realisation.) In a way, the sampling effects of the CT model are automatically modelled in the DT response and are thus easier to analyse.

The frequency-domain characteristics of fractional SRC can be conveniently analysed using image response combining, which is defined for the DT model in [10]. The corresponding CT algorithm is currently under development.

The DT model is easy to handle because the frequency response can be computed numerically from the impulse response. The CT model, on the other hand, requires a more analytic approach, and the formulae for the frequency response are rather complicated [2, Appendix A.1][11]. Furthermore, numerical sensitivity problems occur and must be overcome in the CT frequency response [11]. On the other hand, numerical sensitivity issues can be expected to arise also in the DT model if L is large.

For DT designs, the useful range of the polynomial degree M is bounded from above by L-1 [9]. When M=L–1, the Farrow coefficients have full control over the impulse response (with the restriction of impulse response symmetry), and the DT-optimised impulse response becomes identical to that of the optimal direct-form FIR filter of the same length NL. Using larger values of M cannot improve the response – they will result in the same DT impulse response or numerical problems in optimisation. This limitation cannot be observed from the CT model. Due to the limit, the polynomial degrees used in the DT design examples are $M_{DT}=\min\{M_{CT}, L_T-1\}$, where M_{CT} is the degree used for the CT design.

In CT optimisation, a saturation phenomenon has been observed [12][13, pp. 49–50]. For any given M (N), a saturation threshold exists for N (M), above which no significant performance improvement is obtained. In DT optimisation, there is an exception: If $M \geq L-1$, the performance will *not* saturate when N is increased. Again, the reason is that full control over the DT impulse response is obtained. Notice that such large degrees are often impractical. The saturation phenomenon still remains for $M < L-1$. [9]

The comparison is summarised in Table 1.

Table 1. Summary of benefits and drawbacks of the CT and DT models.

CT model	DT model
+ Robust against changes of L especially at large values	+ Optimal for target L in rational SRC + At large target L, approaches the robustness of CT results – Multi-L optimisation is slow
+ Works for irrational and asynchronous SRC	– Only for rational (including integer) SRC
– Analysis of alias and image attenuation: • How to choose analysis bandwidth?	+ Easier analysis of alias and image attenuation: • Fast, through time-domain image response combining
– Conceals some properties in rational SRC.	+ Reveals importance of sampling phase. + Reveals upper bound for M and saturation properties of N in rational SRC.
– Complicated formulae	+ Easy formulae
– Numerical problems	+ No observed numerical problems – Direct numerical computation of freq. response may be slow and inaccurate for large L.

5. CONCLUSIONS

At large values of target L, DT and CT designs are almost identical. These designs perform well at values of L above some threshold. For smallest values of L, DT optimisation should be used, and the same value of L should be used in optimisation and realisation. In order to make a trade-off between optimality and robustness, we propose a multi-L_T or hybrid DT/CT design approach. A wide range of large values of L_R can be handled by CT criteria or with a single large value of L_T. Small values of L each need optimisation criteria of their own. Unfortunately, multi-L criteria can lead to long optimisation times.

Because the attenuation loss is significant only at small values of L and K<L, it can be concluded that the CT frequency response can be used as a sufficiently accurate approximation for the DT response in most practical rational SRC applications. On the other hand, the CT model can be replaced with a DT model with a large L_T.

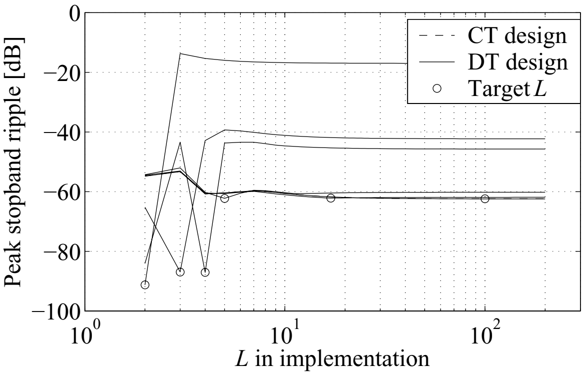

Fig. 6. Stopband attenuation; f_p=0.2, multiple stopbands, N=3, M=min{L_R–1,2}.

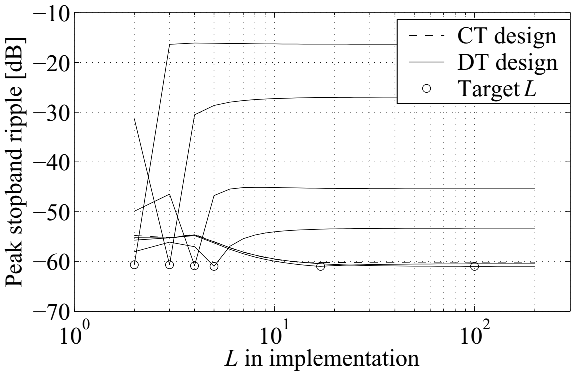

Fig. 7. Stopband attenuation: f_p=0.8, continuous stopband, N=14, M=min{L_R–1,4}.

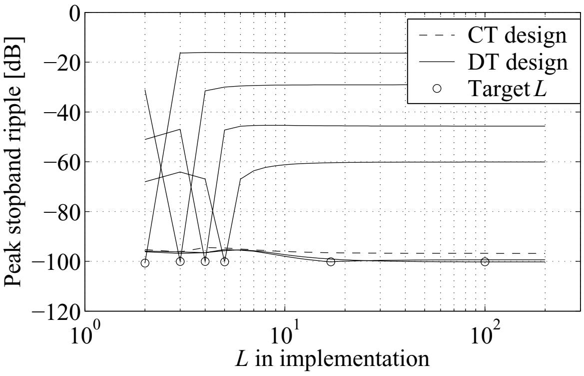

Fig. 8. Stopband attenuation: f_p=0.8, continuous stopband, N=20, M=min{L_R–1,6}.

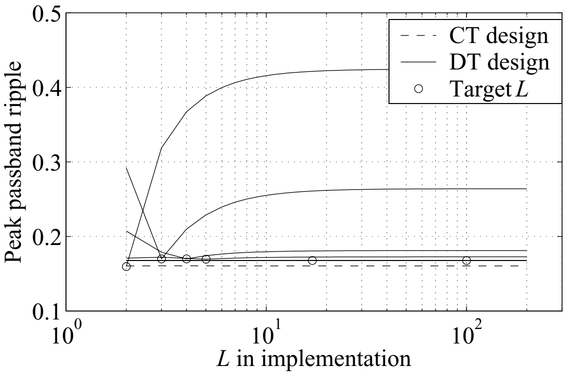

Fig. 9. Passband ripple: f_p=0.8, continuous stopband, N=20, M=min{L_R–1,6}.

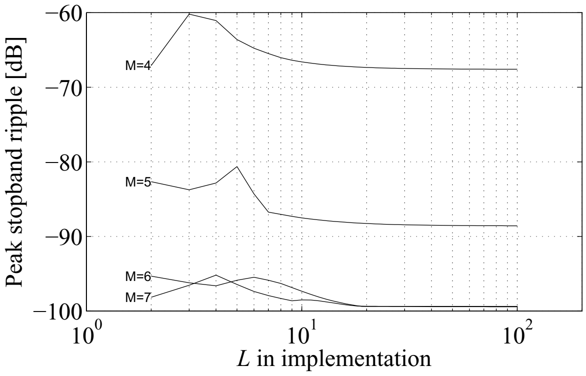

Fig. 10. CT stopband attenuation at different polynomial degrees: f_p=0.8, continuous stopband, N=20.

REFERENCES

[1] R.E. Crochiere, L.R. Rabiner, *Multirate Digital Signal Processing*. Prentice-Hall, 1983.

[2] J. Vesma, *Optimization and Applications of Polynomial-Based Interpolation Filters*, Doctoral dissertation, Department of Information Technology, Tampere University of Technology, Finland, 1999.

[3] C.W. Farrow, "A Continuously Variable Digital Delay Element," in *Proc. IEEE Int. Symp. Circ. Syst.* (*ISCAS*), Espoo, Finland, June 1988, pp. 2641–2645.

[4] T. Hentschel, G. Fettweis, "Continuous-Time Digital Filters for Sample-Rate Conversion in Reconfigurable Radio Terminals," in *Proc. European Wireless*, Dresden, Germany, Sep 2000, pp. 55–59.

[5] D. Babic, J. Vesma, T. Saramäki, M. Renfors, "Implementation of the Transposed Farrow Structure," in *Proc. IEEE Int. Symp. Circ. Syst.* (*ISCAS*), May 2002, pp. IV-5–IV-8.

[6] T. Hentschel, *Multirate Systems for Sample Rate Conversion in Software Radio Terminals*, Doctoral dissertation, Department of Electrical Engineering and Information Technology, Dresden University of Technology, Germany, Sep. 2001.

[7] W.H. Yim, "Distortion Analysis for Multiplierless Sampling Rate Conversion Using Linear Transfer Functions," *IEEE Signal Proc. Letters*, Vol. 8, No. 5, May 2001, pp. 143–144.

[8] D. Babic, V. Lehtinen, M. Renfors, "Discrete-time Modeling of Polynomial-based Interpolation Filters in Rational Sampling Rate Conversion", in *Proc. IEEE Int. Symp. Circ. Syst.* (*ISCAS*), Bangkok, Thailand, May 2003, pp. IV-321–IV-324.

[9] V. Lehtinen, D. Babic, M. Renfors, "On Impulse Response Symmetry of Farrow Interpolators in Rational Sample Rate Conversion", accepted to *First Int. Symp. on Control, Comm. and Signal Proc. (ISCCSP)*, Hammamet, Tunisia, Mar 2004.

[10] V. Lehtinen, M. Renfors, "Analysis of Rational Sample Rate Conversion Using Image Response Combining", in *Proc. IEEE Int. Symp. Circ. Syst. (ISCAS)*, Bangkok, Thailand, May 2003, pp. IV-325–IV-328.

[11] J. Vesma, T. Saramäki, "Polynomial-Based Interpolation Filters–Part I: Filter Synthesis," to appear in *IEEE Trans. Circ. Syst.*

[12] J. Vesma, T. Saramäki, "Polynomial-Based Interpolation Filters–Part II: Filter Properties and Applications," to be submitted to *IEEE Trans. Circ. Syst*.

[13] T. Saramäki, "Polynomial-Based Interpolation for Digital Signal Processing and Telecommunications Applications," lecture notes, Institute of Signal Processing, Tampere University of Technology, Tampere, Finland, Nov 2002 [cited Feb 27, 2004]. Available: http://www.cs.tut.fi/~ts/TapBelgrade.pdf